A continuum model for hydrogen diffusion in a hollow cylinder

Fernando P. Duda, Nélio Achão Filho
Universidade Federal do Rio de Janeiro - COPPE - PEM, Rio de Janeiro – Brazil
Angela C. Souza, Leandro S. Costa
Universidade Federal Fluminense - TEM - PGMEC, Rio de Janeiro – Brazil

Abstract

This paper presents the formulation of a coupled continuum model for deformation and solute diffusion applied in a cylindrical geometry. The formulation is carried out within the framework of the multifield continuum mechanics, where, in addition to the standard fields, extra fields are introduced in order to describe diffusion processes. The theory is singled out and subjected to a numerical implementation based on the finite element method, backward Euler scheme and an operator-split algorithm. A numerical example is given to illustrate the capabilities of the theory to describe the process of constant surface potential.

Keywords: multifield continuum mechanics, solute diffusion in solids.

1 Introduction

In 1878 [1] introduced the idea of a solid which also contains fluid components, whereby a fluid can enter into, move independently through and distort the solid, which otherwise is conserved and behaves elastically. As indicated by [2], a genuine example of this kind of body is provided by interstitial solid solutions at sufficiently low temperatures, with host and interstitial species playing the role of solid and fluids, respectively. Additional examples can be found in the fields of geology, polymer science and metallurgy, as pointed out by [3], who extended Gibbs' idea by allowing solid diffusion. This extension is basic for the modern understanding of equilibrium and diffusion kinetics in solid solutions under stress (see [4] and [5]) as well as for the unified treatment of atomic transport given by [6] (see also [7]).

Particularly, hydrogen in metals provides a large topic of material science, which has attracted considerable interest due to its several applications, such as palladium and palladium-alloy membranes used for hydrogen separation and purification, as described by [8]. These membranes provide this efficient application based on the high solubility and very fast diffusion of the hydrogen in metal-

Mechanics of Solids in Brazil 2009, H.S. da Costa Mattos & Marcílio Alves (Editors)
Brazilian Society of Mechanical Sciences and Engineering, ISBN 978-85-85769-43-7

hydrogen systems. The experiments are generally performed by using tubular membranes, where the initiations of permeation is obtained by gaseous atmospheres of hydrogen at the external surface. [9] have investigated the effect of chemical stress on diffusion in a hollow cylinder for plane strain case, and [10] have concluded that the geometric approximation of modeling thin cylindrical membranes as planar structures fails in the presence of stress-induced diffusion. Some specific boundary conditions have been investigated in the diffusion-induced stress in a hollow cylinder by [11].

Specifically, the purpose of this work is to present a framework based on the formalism of continuum mechanics for the description of solute diffusion, solid-induced deformation applied in a cycilindrical geometry. In accordance with the formalism of modern continuum mechanics (see [6]), we elaborate the framework by introducing the following ingredients: basic balances; free energy imbalance (the second law of thermodynamics) and constitutive theory. We consider as basic the balances of mass for solid and solute, and the balances of forces conjugated to the selected independent kinematical fields, namely solid displacement, solute flow and solute density. The free energy imbalance accounts for energy inflow due to both power expended by all external forces and solute supply, a contribution through which the chemical potential is introduced. The constitutive theory is based upon the following assumptions: additive decomposition of the solid strain into its elastic and solute-induced parts; the dissipation is due degradation and diffusion; the set of constitutive variables includes elastic strain and solute density. Finally, the underlying governing equations of the framework are obtained by merging the aforementioned ingredients. In particular, the equation for the solute flux follows from the corresponding conjugated force balances, whereas the equation for the chemical potential follows from the solute density conjugated force balance.

The present development is similar to that used by [12] in that the solute density and solute flow are considered as independent kinematical descriptors. In particular, the use of the solute density as an independent degree of freedom was inspired on [13] (see also [14]). A preliminary version of this work was presented by the authors in [15].

2 The continuum model

2.1 Preliminaries

Let us consider a continuum hollow cylinder $\mathcal{C}$ with inner radius R_i, outer radius R_e and lenght L. The cylindrical coordinates system standard are (r, θ, z), but for simplicity the hollow cylinder can be treated as an one-dimensional problem, so that we consider only the radial coordinate r.

Therefore, a generic scalar field quantity $\alpha(r,t)$ has temporal derivative denoted by: $\dot{\alpha} := \dfrac{\partial \alpha}{\partial t}$ and its gradient is defined as: $\nabla\alpha := \dfrac{\partial \alpha}{\partial r}\,\mathbf{e}_r$, where $\mathbf{e}_r$ is the unity vector in the radial direction.

A generic vector field $\mathbf{v}(r,t)$, defined as: $\mathbf{v}(r,t) := v(r,t)\,\mathbf{e}_r$, has the temporal derivative given by: $\dot{\mathbf{v}} := \dfrac{\partial v}{\partial t}\,\mathbf{e}_r$, and its gradient is given by:

$$\nabla \mathbf{v} := \begin{bmatrix} \dfrac{\partial v}{\partial r} & 0 & 0 \\ 0 & \dfrac{v}{r} & 0 \\ 0 & 0 & 0 \end{bmatrix} \tag{1}$$

and the divergence is given by:

$$\operatorname{Div} \mathbf{v} := \frac{\partial v}{\partial r} + \frac{v}{r} \tag{2}$$

A generic tensor field $\mathbf{S}(r,t)$ is given by:

$$\mathbf{S} := \begin{bmatrix} S_r & 0 & 0 \\ 0 & S_\theta & 0 \\ 0 & 0 & S_z \end{bmatrix} \tag{3}$$

and the divergence is given by:

$$\operatorname{Div} \mathbf{S} := \begin{bmatrix} \dfrac{\partial S_r}{\partial r} + \dfrac{S_r - S_\theta}{r} \\ 0 \\ 0 \end{bmatrix} \tag{4}$$

We consider that $\mathcal{C}$ contains two components, one that is conserved and acts as a framework through which the other moves independently. For definiteness we name them solid and solute, respectively, whose densities per unit lattice volume are denoted by $\rho_S(r,t)$ and $\rho(r,t)$. For posterior reference we define the solute concentration c as:

$$c := \frac{\rho}{\rho_S}. \tag{5}$$

Besides, the solid can undergo deformation, described by strain tensor field $\mathbf{E}(r,t)$ and the displacement field $\mathbf{u}(r,t) := u(r,t)\,\mathbf{e}_r$, given by:

$$\mathbf{E} := \frac{1}{2}(\nabla \mathbf{u} + \nabla \mathbf{u}^T) \quad \longrightarrow \quad \begin{bmatrix} E_r & 0 & 0 \\ 0 & E_\theta & 0 \\ 0 & 0 & 0 \end{bmatrix} := \begin{bmatrix} \dfrac{\partial u}{\partial r} & 0 & 0 \\ 0 & \dfrac{u}{r} & 0 \\ 0 & 0 & 0 \end{bmatrix} \tag{6}$$

2.2 Basic laws

Since the solid is conserved, it follows from its mass balance that $\dot{\rho}_S = 0$. Therefore we assume henceforth that ρ_S is given. On the other hand, the mass balance for the solute yields the local field equation:

$$\dot{\rho} = -\mathrm{Div}\,\mathbf{J} + h, \tag{7}$$

where $\mathbf{J}$ is the vector field that represents the solute flux and h the external solute supply. The latter is assumed to be given but otherwise arbitrary.

Now we use the principle of virtual to power to obtain the field equations and the boundary conditions corresponding to the basic force balances of the theory. Firstly, we have to decide on which kinematical description to be adopted and then to prescribe two functionals, namely the virtual power of the external forces and the virtual power of the internal forces ([16]). These are considered below.

We consider $\mathbf{u}$, ρ and $\mathbf{J}$ as independent kinematical descriptors and, for a fixed time, we define a generalized virtual velocity $\bar{\mathbf{v}}$ as the list $(\bar{\mathbf{u}}, \bar{\rho}, \bar{\mathbf{J}})$ of smooth time independent fields on $\mathcal{C}$. The set of virtual velocities is denoted by $\mathcal{V}$, which is assumed to contain the realizable velocity $\mathbf{v} = (\dot{\mathbf{u}}, \dot{\rho}, \mathbf{J})$. We remark that $\mathbf{J}$ is a rate-type variable.

For any part $\mathcal{P} = (R_1, R_2)$ of $\mathcal{C}$ we adopt the following prescriptions for the virtual power of the external and internal forces expended on an arbitrary virtual velocity $\bar{\mathbf{v}}$:

- Virtual power of the external forces

$$P_e(\mathcal{P}, \bar{\mathbf{v}}) := \int_{\mathcal{P}} \mathbf{s}^e \cdot \bar{\mathbf{v}}\, dV + \int_{\partial\mathcal{P}} \mathbf{t} \cdot \bar{\mathbf{v}}\, dA, \tag{8}$$

  where the smooth vector fields $\mathbf{t}$ and $\mathbf{s}^e$ describe contact and body interactions, respectively. The infinitesimal quantities are: $dV := r\, dr\, d\theta\, dz$ and $dA := (R_i \text{ or } R_e)\, d\theta\, dz$.

- Virtual power of the internal forces

$$P_i(\mathcal{P}, \bar{\mathbf{v}}) := -\int_{\mathcal{P}} \left(\mathbf{S} \cdot \nabla\bar{\mathbf{v}} + \mathbf{s}^i \cdot \bar{\mathbf{v}}\right) dV, \tag{9}$$

  where the smooth tensor field $\mathbf{S}$ and vector field $\mathbf{s}^i$ describe internal interactions.

The four-tuple lists of quantities denoted by $\mathbf{S} = (\mathbf{T}, \Gamma, \Lambda)$, $\mathbf{s}^i = (\mathbf{b}^i, \gamma^i, \lambda^i)$ and $\mathbf{s}^e = (\mathbf{b}^e, \gamma^e, \lambda^e)$ are related to the fields $\mathbf{u}$, ρ and $\mathbf{J}$, respectively. The Principle of Virtual Power (see, for instance, [16]) states that for each part $\mathcal{P}$:

$$P_i(\mathcal{P}, \bar{\mathbf{v}}) + P_e(\mathcal{P}, \bar{\mathbf{v}}) = 0 \quad \forall\, \bar{\mathbf{v}} \in \mathcal{V}. \tag{10}$$

The above statement in addition with standard arguments, furnishes the field equation:

$$\mathrm{Div}\mathbf{S} - \mathbf{s}^i + \mathbf{s}^e = \mathbf{0} \text{ in } \mathcal{C} \quad \mathbf{s} = \mathbf{S}\mathbf{n} \text{ in } \partial\mathcal{C}, \tag{11}$$

with the understanding that above equations hold componentwise. Therefore, we arrive at the following set of force balances with the corresponding field equations:

- displacement-conjugated force balance

$$\mathrm{Div}\mathbf{T} - \mathbf{b}^i + \mathbf{b}^e = \mathbf{0} \ \text{ in } \mathcal{C} \quad \mathbf{t} = \mathbf{T}\mathbf{n} \ \text{ in } \partial\mathcal{C}, \tag{12}$$

where $\mathbf{T}$, $\mathbf{b}^e$ and $\mathbf{b}^i$ are the motion conjugated stress tensor, external body force and internal body force, respectively, whereas $\mathbf{t}$ is the tractions at the boundary of $\mathcal{C}$. It can be shown that $\mathbf{b}^i$ is equal to zero since the internal power must be frame invariant;

- solute-conjugated force balance

$$\mathrm{Div}\Gamma - \gamma^i + \gamma^e = 0 \ \text{ in } \mathcal{C} \quad \gamma = \Gamma \cdot \mathbf{n} \ \text{ in } \partial\mathcal{C}, \tag{13}$$

where Γ, γ^e and γ^i are the solute density conjugated stress vector, external body force and internal body force, respectively, whereas γ is the tractions at the boundary of $\mathcal{C}$;

- flux-conjugated force balance

$$\mathrm{Div}\Lambda - \lambda^i + \lambda^e = \mathbf{0} \ \text{ in } \mathcal{C} \quad \lambda = \Lambda\mathbf{n} \ \text{ in } \partial\mathcal{C}, \tag{14}$$

where Λ, λ^e and λ^i are the flux conjugated stress tensor, external body force and internal body force, respectively, whereas λ is the tractions at the boundary of $\mathcal{C}$;

2.2.1 Free energy imbalance

We also consider as basic a mechanical version of the second law of thermodynamics, namely the free energy imbalance. It asserts that (see [6]):

$$\frac{d}{dt}\int_{\mathcal{P}} \psi \, dV \leq P_e(\mathcal{P}, \mathbf{v}) + \int_{\mathcal{P}} \mu h \, dV, \tag{15}$$

where ψ is the free energy density, $P_e(\mathcal{P}, \mathbf{v})$ the power expended by all external forces and μ is the chemical potential. After using the principle of virtual power, this version localizes into the dissipation inequality:

$$\dot{\psi} \leq \mathbf{T} \cdot \dot{\mathbf{E}} + \Gamma \cdot \nabla\dot{\rho} + (\gamma^i + \mu)\,\dot{\rho} + (\Lambda + \mu\mathbf{I}) \cdot \nabla\mathbf{J} + \lambda^i \cdot \mathbf{J} \tag{16}$$

3 Constitutive theory

The first constitutive assumption adopted here is the additive decomposition of the strain $\mathbf{E}$,

$$\mathbf{E} = \mathbf{E}_e + \mathbf{E}_s, \tag{17}$$

into its elastic $\mathbf{E}_e$ and solute induced $\mathbf{E}_s$ parts, the latter given by:

$$\mathbf{E}_s = \eta\,(c - c_r)\mathbf{I}, \tag{18}$$

where η is a positive parameter and c_r a reference concentration. It follows then that the dissipation inequality (16) can be written as:

$$\dot{\psi} \leq \mathbf{T} \cdot \dot{\mathbf{E}}_e + \Gamma \cdot \nabla\dot{\rho} + \left(\gamma^i + \mu + \frac{\eta \operatorname{tr} \mathbf{T}}{\rho_S}\right) \dot{\rho} + (\Lambda + \mu\mathbf{I}) \cdot \nabla\mathbf{J} + \lambda^i \cdot \mathbf{J} \tag{19}$$

Based on the inequality (16), we consider constitutive equations of the form:

$$\psi = \hat{\psi}(\mathsf{p}), \quad \mathbf{T} = \hat{\mathbf{T}}(\mathsf{p}), \quad \Gamma = \hat{\Gamma}(\mathsf{p}), \quad \gamma^i + \mu + \frac{\eta \operatorname{tr} \mathbf{T}}{\rho_S} = \hat{\gamma}(\mathsf{p}), \quad \Lambda + \mu\mathbf{I} = \hat{\Lambda}(\mathsf{p}), \quad \lambda^i = \hat{\lambda}^i(\mathsf{p}), \tag{20}$$

where p represents the list of constitutive variables. We assume that:

$$\mathsf{p} := (\underbrace{\mathbf{E}_e, \rho}_{\mathsf{e}}, \mathbf{J}) \tag{21}$$

where e and $\mathbf{J}$ stand for equilibrium and non-equilibrium, or dissipative, variables. We assume that the response functions in (20) are smooth.

Following the Coleman-Noll procedure (see, for instance, [17]), we require that the constitutive responses must be such that the dissipation inequality (16) holds identically for whatever $(\dot{\mathsf{e}}, \dot{\mathbf{J}}, \nabla\dot{\rho}, \nabla\mathbf{J})$ at whatever $(\mathsf{e}, \mathbf{J})$. Hence we conclude that:

- the constitutive function $\hat{\psi}$ is independent of the non-equilibrium variable $\mathbf{J}$, i.e., $\hat{\psi}(\mathsf{e}, \mathbf{J}) = \hat{\psi}(\mathsf{e})$;
- the equilibrium relations

$$\hat{\mathbf{T}} = \frac{\partial\hat{\psi}}{\partial\mathbf{E}_e}, \quad \hat{\Gamma} \equiv 0, \quad \hat{\gamma} = \frac{\partial\hat{\psi}}{\partial\rho}, \quad \hat{\Lambda} \equiv 0 \tag{22}$$

  hold;
- the internal dissipation inequality

$$\hat{\lambda}^i(\mathsf{p}) \cdot \mathbf{J} \geq 0 \tag{23}$$

  must hold for whatever $\mathbf{J}$.

Therefore, the constitutive theory is characterized by the constitutive functions $\hat{\psi}$ and $\hat{\lambda}^i$. The former is independent of $\mathbf{J}$, whereas the later must comply with (23).

The cylinder is considered in a fixed reference configuration at uniform temperature T with constant value for the solid density ρ_S. The densities ρ_S and ρ are given in terms of number of atoms or molecules per unit lattice volume, consequently, the solute concentration $c = \dfrac{\rho}{\rho_S}$ is measured in number of solute atoms per number of solid atoms. Hence, we assume the following free energy and dissipative response:

i) Free energy response:

$$\hat{\psi}(\mathbf{E}_e, \rho) = \frac{\bar{\lambda}}{2}(\operatorname{tr} \mathbf{E}_e)^2 + \bar{\mu}|\mathbf{E}_e|^2 + k_B T \rho \left(\ln\left(\frac{\rho}{\rho_S}\right) - 1\right), \tag{24}$$

where the first two terms correspond to the classical elastic strain energy, and $\bar{\lambda}$ and $\bar{\mu}$ are the Lame parameters. The last term represents the classical entropic contribution to the free energy of a dilute ideal interstitial solid solution, where k_B is Boltzmann's constant and T is the absolute temperature.

ii) Dissipative response:

$$\hat{\lambda} = \frac{1}{M\rho}, \tag{25}$$

where the positive parameter M is the solute mobility.

4 Governing equations

Henceforth we consider the notation for the hollow cylinder as described in the Preliminaries Section, and we assume that $\gamma^e = \lambda^e = 0$. The governing equations for the fields u, μ, ρ and J are obtained through the combination of the aforementioned basic balances and constitutive theory. We also consider the previous definitions related with the gradient and divergent of the scalar, vector and stress fields.

Remark the following relations:

$$E_r = \frac{\partial u}{\partial r}, \quad E_\theta = \frac{u}{r}, \quad c = \frac{\rho}{\rho_S}, \quad D = M\, k_B\, T, \tag{26}$$

where D is the diffusion coeficient.

- The equation for the displacement u is the following:

$$\frac{\partial T_r}{\partial r} + \frac{T_r - T_\theta}{r} + b^e = 0, \tag{27}$$

where:

$$\begin{aligned} T_r &= \bar{\lambda}\,(E_r + E_\theta) + 2\bar{\mu}E_r - \eta(3\bar{\lambda} + 2\bar{\mu})(c - c_r), \\ T_\theta &= \bar{\lambda}\,(E_r + E_\theta) + 2\bar{\mu}E_\theta - \eta(3\bar{\lambda} + 2\bar{\mu})(c - c_r), \\ T_z &= \bar{\lambda}\,(E_r + E_\theta) - \eta(3\bar{\lambda} + 2\bar{\mu})(c - c_r), \end{aligned} \tag{28}$$

- The equation for the chemical potential μ is the following:

$$\mu = k_B T \ln c - \frac{\eta\,(T_r + T_\theta + T_z)}{\rho_S} \tag{29}$$

- the equation for the solute flux J is the following:

$$J = -D\frac{\partial \rho}{\partial r} + \frac{D\,\eta}{k_B T \rho_S}\rho\frac{\partial}{\partial r}(T_r + T_\theta + T_z) \tag{30}$$

- the equation for the solute density ρ is the following:

$$\dot{\rho} = -\frac{\partial J}{\partial r} - \frac{J}{r} + h, \tag{31}$$

with J given by (30).

Observe that, from (29), the chemical potential depends on the solute density and the hydrostatic stress. From (30), we can observe a generalization of Ficks Law, since the solute flux may be driven by the solute density and stress gradients. The prescription of μ implies the prescription of ρ, and vice versa. As pointed out by [4] and [5], when chemical equilibrium prevails at the boundary a constant value for the chemical potential must be prescribed. This does not mean a constant value for ρ, since by (29) the chemical potential may involve not only ρ but also stress and elastic strain.

With the above assumptions, the linear elasticity coupled with the diffusion problem can be stated as follows:

Problem:

Given: Boundary/initial conditions, material and geometrical parameters, body force density, external solute supply and reference concentration,

Find: The displacement u and the solute density ρ, satisfying the following equations:

$$\begin{cases} \dfrac{\partial T_r}{\partial r} + \dfrac{T_r - T_\theta}{r} + b^e = 0, \\ \dot{\rho} + \dfrac{\partial J}{\partial r} + \dfrac{J}{r} = h, \end{cases} \tag{32}$$

where:

$$\begin{aligned} T_r &= \bar{\lambda}\,(E_r + E_\theta) + 2\bar{\mu} E_r - \eta(3\bar{\lambda} + 2\bar{\mu})\left(\frac{\rho}{\rho_S} - c_r\right), \\ T_\theta &= \bar{\lambda}\,(E_r + E_\theta) + 2\bar{\mu} E_\theta - \eta(3\bar{\lambda} + 2\bar{\mu})\left(\frac{\rho}{\rho_S} - c_r\right), \\ J &= -D\frac{\partial \rho}{\partial r} + \frac{D\,\eta}{k_B T \rho_S}\rho\,\frac{\partial (T_r + T_\theta + T_z)}{\partial r}. \end{aligned} \tag{33}$$

The equation for the stress components $(33)_{1,2,3}$ show that stress-assisted diffusion favors solute migration from lower to higher stressed locations. The relation $(33)_3$ shows that diffusion is driven by the solute concentration and hydrostatic stress, then the solute flows from a region of higher to a region of lower concentration. The opposite effect occurs with respect to hydrostatic stress.

Based on the above equations (32), the treatment of boundary conditions at ends $r = R_i$ and $r = R_e$ would be the following: for the equation $(32)_1$, the boundary condition involves the prescription of the displacement or traction, and the boundary condition associated to the equation $(32)_2$ involves the prescription of either ρ or J. Actually, in this article, the bondary contitions related with the force balance equation $(32)_1$ are standard. Therefore, for the solute density equation $(32)_2$ we have considered the chemical potential μ constant at both surfaces. However, because the chemical potential depends explicitly on the trace of stress (see equation (29)), that envolves its dependency on the solute concentration field, the boundary condition for this equation is time dependent.

5 Weak form

Now we briefly describe the steps involved in the construction of the numerical model, which is based on the finite element method, backward Euler scheme and an operator-split algorithm.

The governing equations (32) in their weak forms, are:

Given: Boundary/initial conditions, material and geometrical parameters, body force density and reference concentration,

Find: u and ρ satisfying the following equations:

$$\begin{aligned} &\int_{R_i}^{R_e} \left(T_r \frac{\mathrm{d}v}{\mathrm{d}r} + T_\theta \frac{v}{r} - b^e v \right) r\,\mathrm{d}r + p_i\,R_i - p_e\,R_e = 0 \quad \forall\ v\ \in\ V^0, \\ &\int_{R_i}^{R_e} \left(J \frac{\mathrm{d}\varphi}{\mathrm{d}r} - \dot{\rho}\varphi + h\varphi \right) r\,\mathrm{d}r + J(R_i)\,R_i - J(R_e)\,R_e = 0 \quad \forall\ \varphi\ \in\ V^0, \end{aligned} \tag{34}$$

where:

V^0 is the appropriate functional space,

p_i and p_e are the internal and external pressure,

$$\begin{aligned} T_r &= \bar{\lambda}\,(E_r + E_\theta) + 2\bar{\mu}E_r - \eta(3\bar{\lambda} + 2\bar{\mu}) \left(\frac{\rho}{\rho_S} - c_r \right), \\ T_\theta &= \bar{\lambda}\,(E_r + E_\theta) + 2\bar{\mu}E_\theta - \eta(3\bar{\lambda} + 2\bar{\mu}) \left(\frac{\rho}{\rho_S} - c_r \right), \\ J &= -D\frac{\partial \rho}{\partial r} + \frac{D\,\eta}{k_B T \rho_S}\rho\,\frac{\partial (T_r + T_\theta + T_z)}{\partial r}. \end{aligned} \tag{35}$$

The solution and test spaces (functional spaces) are approximated by finite dimensional spaces by using the finite element method. The approximated fields are denoted by u_h, ρ_h, v_h and φ_h.

$$\begin{aligned} &\int_{R_i}^{R_e} \left((T_r)_h \frac{\mathrm{d}v_h}{\mathrm{d}r} + (T_\theta)_h \frac{v_h}{r} - (b^e)_h\,v_h \right) r\,\mathrm{d}r + (p_i)\,R_i - (p_e)\,R_e = 0, \\ &\int_{R_i}^{R_e} \left(J_h \frac{\mathrm{d}\varphi_h}{\mathrm{d}r} - \dot{\rho}_h\,\varphi_h + h_h\,\varphi_h \right) r\,\mathrm{d}r + J(R_i)\,R_i - J(R_e)\,R_e = 0. \end{aligned} \tag{36}$$

Or, in a simplified notation, we have the following semi-discrete systems of equations that represent the system in (36):

$$
\begin{aligned}
&\mathbf{F}_u(\mathbf{u}, \rho) = \mathbf{0} \\
&\mathbf{F}_\rho(\mathbf{u}, \rho, \dot{\rho},) = \mathbf{0}
\end{aligned}
\tag{37}
$$

where $\mathbf{u}$ and ρ are vectors containing the unknown nodal values for u_h and ρ_h . The functions $\mathbf{F}_u$ and $\mathbf{F}_\rho$, viewed as vector valued, have the same dimensions of $\mathbf{u}$ and ρ , respectively. The temporal discretization of this set of equations is carried out by using the Euler implicit method. This results in the following set of equations for each time instant t_k:

$$
\begin{aligned}
&\mathbf{F}_u(\mathbf{u}^k, \rho^k) = \mathbf{0}, \\
&\mathbf{F}_\rho(\mathbf{u}^k, \rho^k, \dot{\rho}^k) = \mathbf{0},
\end{aligned}
\tag{38}
$$

where, for a time dependent function f, f^k and $\dot{f}^k$, which is given by:

$$
\dot{f}^k = \frac{f^k - f^{k-1}}{t_k - t_{k-1}}, \tag{39}
$$

are approximations to $f(t_k)$ and $\dot{f}(t_k)$, respectively.

The computational problem is to determine $\mathbf{u}^k$ and ρ^k given ρ^{k-1}. This is solved by using a staggered scheme comprising the following steps:

i) assume ρ^{k-1} as trial solutions for ρ^k;

ii) obtain the trial solution for $\mathbf{u}^k$ by solving $(38)_1$;

iii) update the trial solution for ρ^k by solving $(38)_2$;

iv) if convergence is attained, update $\mathbf{u}^k$ and ρ^k using their trials, otherwise, go to Step (ii) repeating the next steps.

Each subproblem is solved for its primitive variable while holding that of the other subproblems equal to their current trials. In the Step (iii), the mechanical stress is obtained from the displacement and concentration through a direct computation followed by nodal averaging.

6 Numerical example

In this section solutions to the initial boundary value problem of transient hydrogen diffusion coupled with elasticity are presented in a hollow cylinder, with inner radius $R_i = 150$ mm and outer radius $R_e = 190$ mm. Plane strain was assumed and the system's temperature was 300 K. The material used in the simulations was high strenght steel and the properties are listed in Table 1 see [18]).

The units used are: the solid density ρ_S is measured in host lattice atoms (Fe) per volume, i.e., (Fe/m^3), and the hydrogen density ρ is measured in hydrogen atoms (H) per volume, i.e., (H/m^3).

The solute concentration $c = \frac{\rho}{\rho_S}$, is, then, measured in hydrogen atoms (H) per host lattice atoms (Fe), i.e., H/Fe.

We assumed that the cylinder is under a prescribed constant pressure on the internal and external surface: $p_i = 100.0\,\text{MPa}$, $p_e = 50.0\,\text{MPa}$, respectively. As well as, the boundary condition for the solute density equation is the constant chemical potential $\mu = -2.0\text{x}10^{-20}$ Joule/H on both surfaces. These conditions were adopted in order to mimic the situation described in [11].

Table 1: Material properties of high strenght steel with internal hydrogen.

$\bar{\lambda}$	119.0 GPa
$\bar{\mu}$	79.0 GPa
D	$1.0\text{x}10^{-8}$ m^2/s
ρ_S	$8.454\text{x}10^{28}$ Fe/m^3
$k_B T$	$4.14\text{x}10^{-21}$ Joule/H
η	0.0937 Fe/H

The displacement field with different times are plotted in Figure 1. The blue line corresponds to initial instant, when the diffusion process had not started, and the cylinder is only under internal and external pressure, and the black line corresponds to the final instant of the simulation.

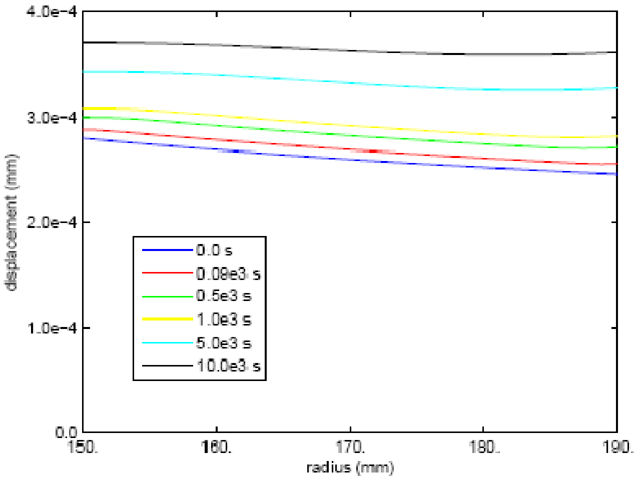

Figure 1: The displacement field

The solute concentration distribution with different times are plotted in Figure 2. Initially no solute atom is in the solid, that corresponds to blue line. The solute diffuses from both outer and inner surfaces into the middle of the cylinder, and then the concentration increases with an increase in time.

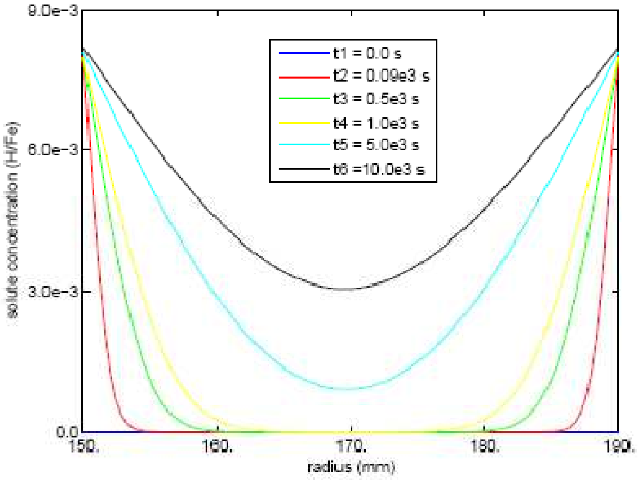

Figure 2: The solute distribution

As shown in Figure 3 the radial stress component is compressive in all instants and everywhere, the curves do not differ significantly and have the maximum value at inner surface whereas the internal pressure is higher than the external pressure.

The circumferential stress component, shown in Figure 4, is tensile everywhere. It is interesting to observe that at the beginning of the process the curves are close the blue one, that represents to initial instant.

Almost the same situation we find in the distribution of the axial stress component, shown in Figure 5, at the beginning of the process the curves are close to the initial instant, and all curves are almost symmetric with respect to the middle of cylinder. This component is compressive in the region near both surfaces and tensile in the middle region of cylinder. The distribution of the trace of the stress is quite similar, but all curves and everywhere the trace corresponds to tensile stress, shown in Figure 6.

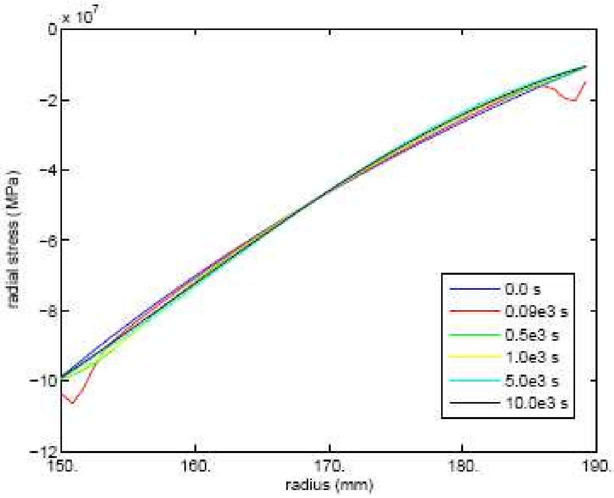

Figure 3: The radial stress component profiles

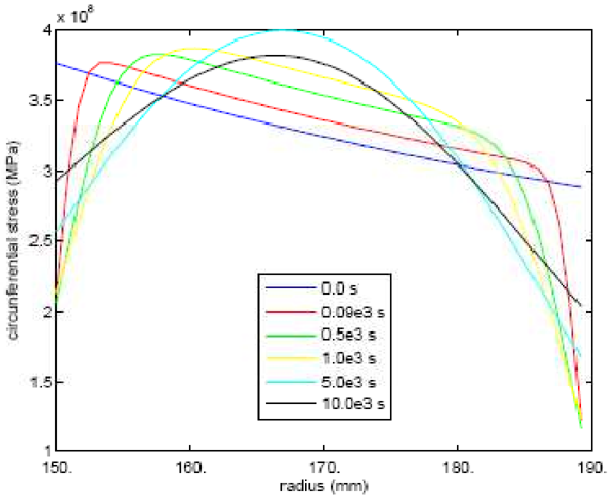

Figure 4: The circumferential stress component profiles

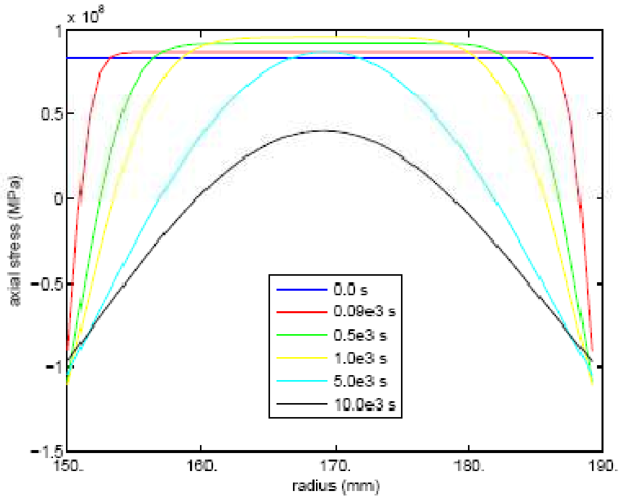

Figure 5: The axial stress component profiles

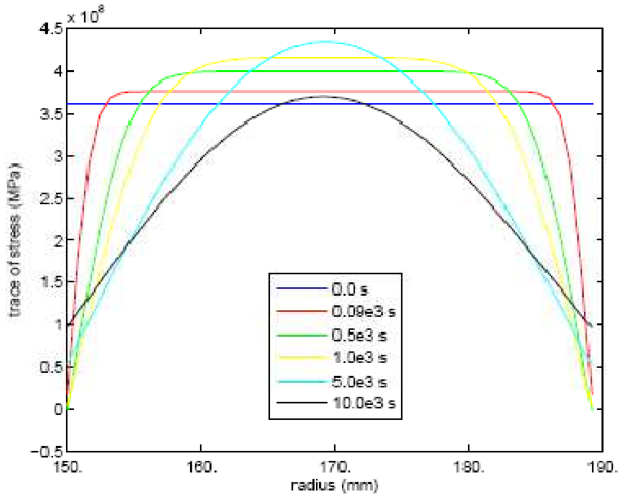

Figure 6: The trace of stress profiles

Acknowledgements

Duda F.P. gratefully acknowledges the support by CNPq (485866/2006-4, 484579/2006-1 and 201080/2008-7) and FAPERJ (E-26/171.599/2004). Souza A.C. gratefully acknowledges the support by the FAPERJ (E-26/170.292/2006) and CAPES (0720/08-9).

References

[1] Gibbs, J.W., *The Scientific Papers of J. Williard Gibbs, Volume One, Thermodynamics*. Ox Bow press, 1993.

[2] Li, J.C.M., Oriani, R.A. & Darken, L.S., The thermodynamics of stressed solids. *Z physik Chem Neue Folg*, **Bd. 49**, pp. 271–290, 1966.

[3] Larché, F.C. & Cahn, J.W., A linear theory of thermochemical equilibrium of solids under stress. *Acta Metallurgica*, **21**, pp. 1051–1063, 1973.

[4] Larché, F.C. & Cahn, J.W., The effect of self-stress on diffusion in solids. *Acta Metallurgica*, **30**, pp. 1835–1845, 1982.

[5] Larché, F.C. & Cahn, J.W., The interactions of composition and stress in crystalline solids. *Acta Metallurgica*, **33**, pp. 331–357, 1985.

[6] Fried, E. & Gurtin, M., Coherent solid-state phase transitions with atomic diffusion: A thermomechanical treatment. *J Statistical Physics*, **95(5-6)**, pp. 1361–1427, 1999.

[7] Fried, E. & Gurtin, M., A unified treatment of evolving interfaces accounting for small deformations and atomic transport with emphasis on grain-boundaries and epitaxy. *Advances in Applied Mechanics*, **40**, pp. 1–177, 2004.

[8] Buxbaum, R.E. & Kinney, A.B., Hydrogen transport through tubular membranes of palladium-coated tantalum and niobium. *Ind Eng Chem Res*, **35**, pp. 530–537, 1996.

[9] Wang, W.L., Lee, S. & Chen, J.R., Effect of chemical stress on diffusion in a hollow cylinder. *J Appl Physics*, **91**, pp. 9584–9590, 2002.

[10] Adrover, A., Giona, M., Capobianco, L., Tripoli, P. & Violante, V., Stress induced diffusion of hydrogen in metallic membranes: cylindrical vs. planar formulation I. *J Alloy and Compounds*, **358**, pp. 268–280, 2003.

[11] Lee, S., Wang, W.L. & Chen, J.R., Diffusion-induced stress in a hollow cylinder. *Mat Sci Eng*, **A285**, pp. 186–194, 2000.

[12] Fried, E. & Sellers, S., Theory for atomic diffusion on fixed and deformable crystal lattices. *J Elasticity*, **59**, pp. 67–81, 2000.

[13] Gurtin, M.E., Generalized Ginzburg-Landau and Cahn-Hilliard equations based on a microforce balance. *Physica D*, **92**, pp. 178–192, 1996.

[14] Podio-Guidugli, P., Models of phase segregation and diffusion of atomic species on a lattice. *Ricerche di Matematica*, **55**, pp. 105–118, 2006.

[15] Duda, F.P., Souza, A.C., aes, L.J.G. & Barbosa, J.M., An one dimensional coupled model for deformation, degradation and solute diffusion in elastic solids. *Mechanics of Solids in Brazil*, eds. M. Alves & H.S. da Costa Mattos, Brazilian Society of Mechanical Sciences and Engineering, 2007.

[16] Germain, P., The method of virtual power in continuum mechanics. part 2: Microstructure. *SIAM J Appl Math*, **25(3)**, 1973.

[17] Silhavy, M., *The Mechanics and Thermodynamics of Continuous Media*. Springer-Verlag: Berlin, 1997.

[18] Taha, A. & Sofronis, P., A micromechanics approach to the study of hydrogen transport and embrittlement. *Eng Fracture Mechanics*, **68**, pp. 803–937, 2001.